Journal of Materials Chemistry A

Accepted Manuscript

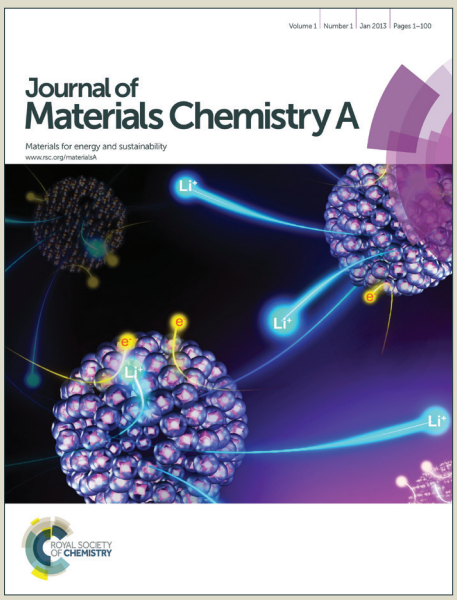

ROYAL SOCIETY OF CHEMISTRY

www.rsc.org/materialsA

Graphical abstract

The proposed nanoreactor was made of Pt nanoparticles and a unique polymer composite of PVI and PTFMA. The self-healing and dissociation of the PVI- PTFMA interaction regulated access to the encapsulated metal nanoparticles, thereby causing self-switchable catalytic ability.

TOC figure:

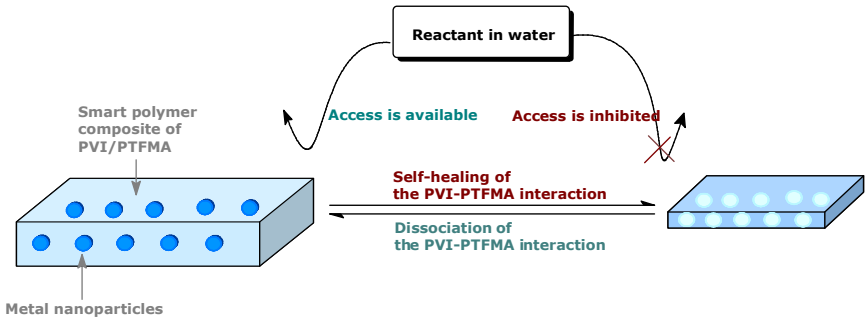

Self-Switchable Catalysis by a Nature-Inspired Polymer Nanoreactor Containing Pt Nanoparticles

Yong Zhou, Maiyong Zhu, Songjun Li*

School of Materials Science & Engineering, Jiangsu University, Zhenjiang 212013, China

Abstract: A nature-inspired polymer nanoreactor with self-switchable catalytic ability is reported. This nanoreactor was made of platinum nanoparticles and a unique polymer composite of poly(1-vinylimidazole) (PVI) and poly(2-(trifluoromethyl)acrylic acid) (PTFMA) that exhibited "self-healing" properties. This nanoreactor revealed weak reactivity at relatively low temperatures due to the complementary interaction between PVI and PTFMA, which inhibited access to the catalytic sites of platinum. In contrast, the nanoreactor demonstrated significant reactivity at relatively high temperatures, resulting from the dissociation of the interpolymer interaction. Unlike reported nanoreactors which usually involve the thermal phase transition of PNIPAm, this novel nanoreactor has adopted the "self-healing" properties of supramolecular building blocks. The proposed design suggests new opportunities for developing smart nanoreactors capable of self-switchable catalysis.

Keywords: Metal nanoparticles; polymer carrier; switchable catalysis

* Corresponding to Prof. S. Li, *Distinguished Professor* to Jiangsu University and *President* of Chinese Advanced Materials Society
Email: Lsjchem@ujs.edu.cn

1. Introduction

Metal nanoparticles are currently the subject of intensive studies, due to their importance in a broad range of applications and in particular in catalytic applications. The recent advances in this field and advanced materials offer new opportunities to develop functional catalysts by incorporating both of them into individual entitles.[1-3] Prominent among them are the switchable nanoreactors, which gain traction due to the tantalizing demand for controlled pathways in chemical synthesis and in inaccessible places. With the earliest endeavors made in developing poly(*N*-isopropylacrylamide) (PNIPAm)-encapsulated Ag nanoparticles,[4,5] the nanoreactors demonstrate tunable catalysis in water, resulting from the thermal phase transition of PNIPAm. The relative balance between the hydrophilic and the hydrophobic properties present in the polymeric building blocks is thus broken, which causes either an impeded or an unobstructed access into the encapsulated Ag nanoparticles. In this way, catalysis by the nanoreactors is recognized as a tunable process. The level of innovative thinking applied to develop functional nanoreactors in the recent years has been high, which may be reflected by the adoption of special polymers or polymeric materials with elaborate structures as the support of metal nanoparticles.[6-10] Nonetheless, the furnishing of catalytic nanoreactors with tunable properties has been proven to be difficult, mainly because most of the reported polymers suitable for supporting metal nanoparticles are not PNIPAm, which lack thermal phase transition and adjustable elements. It is also practically complicated and challenging to fabricate polymeric supports containing elaborate structures. As such, the appeal for new protocols suitable for the general development of nanoreactors remains high.

For centuries, mankind has been learning and achieving knowledge from nature. A body of knowledge is already available. Scientists have learnt to create and resolve complicated scientific problems through the inspiration sought from nature. One of them is the self-healing materials, which were earliest suggested by White, Moore and co-workers[11,12] and intended for repairing cracks. To the end, microcapsules containing unreacted monomers were embedded in a thermoset matrix dispersed with catalysts. When a crack formed, the capsules were broken and the monomers

were thus released and then exposed to the catalysts, causing polymerization and cracks self-repairing. The recent development in this field have brought up a large number of self-healing materials and mechanisms.[13,14] Nonetheless, the simplest one can be the supramolecular self-healing polymers, such as poly(ethylenimine-co-acrylic acid),[15] which are held together by hydrogen-bonding interactions. The self-healing is reversible due to the reversibility of the hydrogen-bonding interactions. The contact between cut surfaces, cracks, and defects would restore these hydrogen-bonding interactions, causing the self-healing of these materials. Although these works are not directly related to catalytic applications, the methods developed by self-healing scientists provide new insight into the stranded catalytic nanoreactors, which makes feasible the switchable interactions.

Inspired by this principle, we herein report a unique nanoreactor equipped with self-switchable catalytic ability (**Scheme 1**). This nanoreactor was made of platinum nanoparticles and a unique polymer composite of poly(1-vinylimidazole) (PVI) and poly(2-(trifluoromethyl)acrylic acid) (PTFMA) that exhibited self-healing interactions.[16] PVI and PTFMA were selected for the fabrication of this nanoreactor, as they can form stronger electrostatic interactions in contrast to the conventional hydrogen-bonding, which allow better control of access to the encapsulated metal nanoparticles. As outlined in **Scheme 1**, the novel nanoreactor (*i.e.*, "PtNR-S") was capable of switchable catalysis due to the complementary interaction between PVI and PTFMA. The self-healing and dissociation of the complementary interaction enabled switchable access to the encapsulated metal nanoparticles, resulting in switchable catalytic ability. In this way, catalysis by this nanoreactor demonstrated a tunable process. The objective of this study is to demonstrate that catalytic nanoreactors equipped with self-switchable catalytic ability can be fabricated by using this novel design, which suggests new opportunities for developing smart catalysts capable of self-switchable catalysis.

Scheme 1. Technical outline for the self-switchable catalysis of PtNP-S

2. Experimental Section

2.1. Preparation of nanoreactors

The chemicals used were of analytic grade and used as received from Sigma-Aldrich (except 1-vinylimidazole (VI) and divinylbenzene (DVB), which were washed with 5 wt% sodium hydroxide solution prior to use[17]). The preparation of the nanoreactor was based on an optimized 2-(trifluoromethyl)acrylic acid) (TFMA)-VI ratio and the details would be discussed afterward. VI (0.52 g) along with TFMA, chloroplatinic acid hexahydrate (0.16 g), AIBN (0.50 g), and a certain amount of DVB (10 wt-%, relative to the sum of monomers)[18] were dissolved in dimethyl sulfoxide (10 mL). After being dispersed and deoxygenated with sonication and nitrogen, the mixture system was irradiated with ultraviolet light (365 nm) overnight. The platinum (IV) ion encapsulated in the resulted polymer was reduced by an excess of sodium borohydride (10 folds, relative to ionic platinum). The resulted nanoreactor (*i.e.*, PtNR-S) was profusely washed with methanol and water, and then dried under flowing nitrogen.

For a comparative study, two controls, *i.e.*, "PtNR-N" and "NR-S", were also prepared under comparable conditions. PtNR-N was the conventional and non-responsive platinum nanoreactor prepared without using TFMA (herein, *N* means 'non-responsive' in contrast to the *S* 'switchable' in PtNR-S). NR-S was the carrier of PtNR-S and prepared without using platinum. For the sake of a convenient discussion, all of the prepared nanoreactors and carrier were mentioned henceforth as the conceptual nanoreactors (but not specified by nanoreactors or carriers).

2.2. TEM and FTIR analysis

The TEM images of the prepared nanoreactors are obtained using a transmission electron microscope (TEM) (JEM-2100, Japan). Samples dispersed in alcohol were placed onto a 200-mesh copper TEM grid (3 mm) (Germany). The infrared spectra were taken in KBr-pressed tablets using a FTIR apparatus (Nicolet MX-1E, USA).

2.3. Self-switchable interactions

The switchable interaction between PVI and PTFMA was studied as a function of temperature

by using dynamic light scattering (DLS) (Bettersize-2000, China). In order to allow for equilibrium reaching, all samples were kept at specified temperatures for at least 10 min before acquiring the hydrodynamic radius (R_h). By a comparison between the switchable nanoreactors (*i.e.*, PtNR-S and NR-S) and the conventional PtNR-N, the contribution of the PVI-PTFMA interaction can be reflected by the relative change of hydrodynamic radius (R_c):[19]

$$R_c = \left[\left(\frac{R_h - R_d}{R_d} \right)_S - \left(\frac{R_h - R_d}{R_d} \right)_N \right] \times 100\% \quad (1)$$

Herein, R_d is the particle size of dried particles. *S* represents the switchable nanoreactors and *N* indicates the non-responsive nanoreactor.

2.4. Catalysis test

The catalytic properties of the prepared nanoreactors were evaluated using the model reaction of reducing sodium fluorescein (SF) with $NaBH_4$.[20] SF was added into $NaBH_4$ aqueous solution with an initial concentration of 0.01 μmol mL^{-1} (totally 3 mL; $NaBH_4$, 20 folds in contrast to SF). The solid content of nanoreactors in the reaction system for each test was 0.06 mg mL^{-1}. The reduction of SF was spectrophotometrically monitored. The catalytic activity of these nanoreactors was obtained from the average of triple runs.

2.5. Electrochemical test

The electrochemical test was further employed to achieve information on the interaction between the prepared nanoreactors and substrate.[21] Using an electrochemical workstation equipped with a three-electrode configuration (Au-plate working electrode, Pt-wire counter electrodes and Ag^+/AgCl ref. electrode) (CHI 760E, China), nanoreactors (10 mg) that pre-absorbed with *ca.* 1 nmoL SF were placed into a cuvette encircled by a diffusion-eliminated sonication apparatus (supporting electrolyte: 0.01 mmol mL^{-1} KCl; 10 mL). The substrate transiently desorbed was cyclic-voltammetrically scanned by the workstation up to a stable desorption/reduction profile achieved (scanning range, +0.6~ -0.4 *V*; scanning rate, 1 m$V \cdot s^{-1}$).

3. Results and Discussion

3.1. PVI-PTFMA interaction and its optimization

As aforementioned, the PtNR-S nanoreactor was capable of switchable catalysis due to the complementary interaction between PVI and PTFMA. The self-healing and dissociation of this complementary interaction enabled switchable access to the encapsulated metal nanoparticles, causing tunable catalysis. An excess amount of either monomer would endow the prepared nanoreactor with steric mismatch between PVI and PTFMA, causing unsaturated interactions and defective association/dissociation. The stoichiometric PVI-PTFMA interaction would help eliminate the unsaturated interactions and is thus in favor of the responsiveness of the resulted polymer.[22] In order to monitor this interaction, the titration of VI with TFMA was conducted. The titration would induce an alteration at the electron-cloud distribution of VI and thus a change in the transition between electronic energy levels, causing shifts in the UV spectrum.[23] As shown in **Figure 1,** the titration of TFMA to VI caused a shift in the UV spectrum and the shift became a maximal value when the titrated TFMA reached a critical amount (corresponding to 1.18 mol/mol TFMA/VI ratio). Beyond the critical amount, no further shift in the UV spectrum was observed (except for increased absorbance). This result suggests that the VI-TFMA interaction was saturated by the stoichiometric titration and the TFMA/VI ratio was thus optimized. Hence, 0.91 g (6.5 mmol) of TFMA was used to prepare the self-switchable PtNR-S and its controls, where 0.52 g (5.5 mmol) of VI was adopted.

Figure 1. The change of UV spectra as a function of TFMA/VI molar ratio
(In which, TFMA (0.2 mmol mL^{-1}; 50 μ L/titration) was titrated into VI (0.03 mol mL^{-1}; 2.5 mL)

3.2. FTIR and TEM analysis

The nanoreactors were thus prepared by using the optimized polymer of PVI/PTFMA as the support of platinum nanoparticles. FTIR and TEM were used to characterize the composition. As shown in **Figure 2**, three major bands (3000-3600, 1550-1800, and 1000-1500 cm^{-1}) appeared in the

spectrum of PtNR-S. These bands are complex due to the complicated composition, which may be associated with the stretching of O-H/N-H, C=O, and C-N/C-C.[24] For a comparative study, we also included two controls (*i.e.*, PtNR-N and NR-S) in **Figure 2**. NR-S revealed almost the same spectrum as PtNR-S, while PtNR-N failed to. Both PtNR-S and NR-S raised a strong absorption peak at 1550-1800 cm^{-1}, compared with PtNR-N. This result may be due to the comparable composition between NR-S and the supporting polymer of PtNR-S. The preparation of PtNR-S and NR-S involved TFMA and thus raised a strong absorption peak of carbonyl group. **Figure 3** presents the TEM images of these nanoreactors. Platinum nanoparticles with the size of about 20-30 nm were encapsulated in the polymeric building blocks. Hence, these nanoreactors were prepared with the expected structures and morphology, which thereby makes feasible a further and comparative study.

Figure 2. FTIR spectra of the prepared nanoreactors

Figure 3. TEM images of the prepared nanoreactors. a) NR-S; b) PtNR-S; c) PtNR-N

3.3. Evaluation of the self-switchable interaction

Figure 4 presents the DLS curves of these prepared nanoreactors. The hydrodynamic radii (R_c) of PtNR-S and NR-S revealed significant dependence upon temperature, relative to PtNR-N. There was a small delay in PtNR-S in contrast to NR-S, a result relating to the presence of metal nanoparticles, which partially restrained the mobility of the supramolecular building blocks. The R_c of PtNR-S and NR-S increased with elevated temperature and the major increase appeared at 38-44 ^{o}C. Below this region, PtNR-S and NR-S revealed a low R_c associating with the interpolymer interaction between PVI and PTFMA, which inhibited the swelling of the polymeric building blocks (**Scheme 1**). In contrast, above this temperature region, the R_c of PtNR-S and NR-S dramatically increased in response to the dissociation of the interpolymer interaction, which caused swelling of the polymeric building blocks. This result suggests the self-switchable properties of

PtNR-S and NR-S, as expected.

Figure 4. DLS curves of the prepared nanoreactors
(In distilled water, with particles concentration of *ca.* 0. 1 μg mL^{-1})

3.4. Switchable catalysis

The catalytic properties of these nanoreactors are presented in **Figure 5**. NR-S did not reveal significant catalysis due to the lack of catalytic platinum nanoparticles (the minor conversion can be due to the self-reduction of SF with $NaBH_4$).[20,22] In contrast, PtNR-S and PtNR-N exhibited significant catalytic ability, where the conversion of SF increased rapidly with time. In order to assess the switchable catalysis, two representative temperatures, *i.e.*, 30 and 50 ^oC (either higher or lower than the thermosensitive region of PtNR-S and NR-S, *i.e.*, 38-44 ^oC), were selected for a contrastive study. At 50 ^oC, PtNR-S exhibited reactivity significantly higher than the conventional PtNR-N. In contrast, at 30 ^oC, PtNR-S revealed weak reactivity, which was lower than PtNR-N. PtNR-S demonstrated switchable catalysis, as expected. This result, as previously explained, can be related to the self-switchable interaction within PtNR-S. The self-healing and dissociation between PVI and PTFMA regulated the access of substrate to the catalytic sites of platinum, which thereby made feasible the switchable catalysis.

Figure 5. Reactivity of the prepared nanoreactors for the reduction of SF
(SF initial concentration, 0.01 μmol mL^{-1}; nanoreactors, 0.06 mg mL^{-1}; $NaBH_4$, 20 folds in contrast to SF)

3.5. Kinetic study of catalysis

For the kinetic study of reducing dye molecules, pseudo-first-order kinetics is commonly used as the modeling means. Since the concentration of the reducing agent $NaBH_4$ largely exceeded SF, the reaction rate could be assumed to be independent of the borohydride concentration. Hence, a pseudo-first-order kinetic study with respect to the SF concentration was conducted to evaluate the catalysis:[25]

$$-\frac{dC}{dt} = kC$$

$$\text{or} \quad -\frac{dx}{dt} = k(1-x) \qquad (2)$$

Herein, C and x are the concentration and conversion of SF at time t, respectively, and k is the rate constant. By further deducing this equation, connecting equation (2) at different temperatures would present the effect of temperature on the catalytic activity of a nanoreactor:

$$\frac{dx_{\mathrm{H}}}{1-x_{\mathrm{H}}} = \frac{k_{\mathrm{H}}}{k_{\mathrm{L}}} \cdot \frac{dx_{\mathrm{L}}}{1-x_{\mathrm{L}}} \quad (3)$$

Here, the subscripts 'L' and 'H' represent the relatively low and high temperatures, respectively. After defining a constant R_r ($\equiv k_{\mathrm{H}}/k_{\mathrm{L}}$) that reflects the relative reactivity, Equation (3) is concluded with Equation (4):

$$\ln(1-x_{\mathrm{H}}) = R_r \ln(1-x_{\mathrm{L}}) \quad (4)$$

The relative reactivity of a nanoreactor at different temperatures is thus linked with the conversion. The R_r-value is available through plotting the function of conversion. As shown in **Figure 6**, the R_r-value in the PtNR-N system did exhibit a good linear correlativity (where the correlative coefficient was as high as 0.9909). The elevated temperature led to increased reactivity in the PtNR-N system (increased by 42%). In contrast, although there were similar increases in the reactivity of PtNR-S, the reactivity did not increase in the same paradigm as PtNR-N (and ran with bending). This result strongly suggests that catalysis by the PtNR-S nanoreactor is a tunable process and which can be tunable with temperature. Once again, this result reflects the self-switchable properties within PtNR-S. The self-healing and dissociation between PVI and PTFMA caused switchable access to the encapsulated metal nanoparticles, which thereby resulted in tunable catalysis.

Figure 6. Kinetic fitting of the catalytic activities of the prepared nanoreactors
(SF initial concentration, 0.01 μmol mL^{-1}; nanoreactors, 0.06 mg mL^{-1})

3.6. Dynamic binding behavior

Electrochemical studies were further conducted to ascertain the mechanism between these nanoreactors and substrate. It is known that the potential to reduce/oxidize a binding molecule depends upon the binding constant. A strong binding will need more energy to overcome the binding, thereby resulting in a larger redox potential. The theory and details, as outlined in **Scheme 2**, have been described elsewhere.[20,26] The substrate (B) in this electrochemical system would normally involve desorption, diffusion to the surface of electrodes, and electrochemical reaction. In the event that the diffusion is eliminated with sonication, the binding constant (K) can be directly corrected to the change of the redox potential (E) (*i.e.*, $\Delta \ln K = a\Delta E$). As such, the electrochemical study on substrate desorbing can provide valuable information on the binding behavior between nanoreactors and substrate. By considering the thermosensitive responsiveness of PtNR-S, which had effects on the catalytic reduction of SF (cf. **Figure 5**), we further selected 30 and 50 ^{o}C for a contrastive study. As shown in **Figure 7**, SF attached to PtNR-S at 30 ^{o}C exhibited a reduction peak at -163 mV. In contrast, the reduction peek at 50 ^{o}C shifted to a smaller position (*i.e.*, -128 mV). As anticipated, PtNR-S demonstrated a stronger interaction with SF at 30 ^{o}C than at 50 ^{o}C. The self-switchable ability appears to play roles for the interaction.

In order to further address this interaction, **Table 1** provides the reduction potentials with substrate desorbing from all of the prepared nanoreactors. Despite the encapsulated platinum nanoparticles, PtNR-S showed the reduction potentials comparable to that of NR-S. Both PtNR-S and NR-S were almost in the same potential change in response to the elevated temperature. In contrast, the conventional PtNR-N did not reveal significant shifts in the reduction potential. This result indicates that the tunable catalysis by PtNR-S is essentially a result of the self-switchable polymer carrier, which regulated access to the catalytic sites of platinum, thereby causing the self-switchable catalysis.

Scheme 2. Schematic presentation of an electrochemical process with the binding molecule B

Figure 7. Reduction profiles with SF desorbing from the prepared nanoreactors (*a*: 30 ^{o}C; *b*: 50 ^{o}C) (Au working electrode, Pt counter electrodes, Ag^{+}/AgCl ref. electrode; supporting electrolyte: 0.01 mmol mL^{-1} KCl).

Table 1. Reduction potentials with SF desorbing from all nanoreactors

4. Conclusions

A nature-inspired nanoreactor capable of self-switchable catalytic ability was prepared and characterized in this study. This nanoreactor was made of platinum nanoparticles and a unique polymer composite of poly(1-vinylimidazole) (PVI) and poly(2-(trifluoromethyl)acrylic acid) (PTFMA). The nanoreactor demonstrated switchable catalysis due to the self-healing properties of the supramolecular building blocks. The self-healing and dissociation between PVI and PTFMA enabled switchable access to the encapsulated metal nanoparticles, which caused self-switchable catalysis. It is thus demonstrated that polymer nanoreactors equipped with self-switchable ability can be realized by using self-healing polymers, which suggests new opportunities for developing smart catalysts. Future development in this field will significantly increase the potential for practical applications, and will lead to the appearance of novel catalytic materials and functional catalysts.

Acknowledgements

The authors want to express their gratitude to both Jiangsu Province and Jiangsu University for supporting this study under the distinguished professorship program (Sujiaoshi [2012]34 and No.12JDG001) and the innovation/entrepreneurship program (Suzutong [2012]19). Thanks should be also expressed to the Science and Technology Agency of Jiangsu Province (BK20130486).

References

1 J. Yuan, S. Wunder, F. Warmuth and Y. Lu, *Polymer*, 2012, **53**, 43-49.

2 F. H. Richter, Y. Meng, T. Klasen, L. Sahraoui and F. Schüth, *J. Catal.*, 2013, **308**, 341-351.

3 W. G. Menezes, V. Zielasek, K. Thiel, A. Hartwig and M. Bäumer. *J. Catal.*, 2013, **299**, 222-231.

4 C. W. Chen, M. Q. Chen, T. Serizawa and M. Akashi, *Adv Mater.*, 1998, **10**, 1122-1126.

5 S. Wu, J. Dzubiella, J. Kaiser, M. Drechsler, X. Guo, M. Ballauff and Y. Lu, *Angew. Chem. Int. Ed.*, 2012, **51**, 2229-2233.

6 Y. Yang, X. Liu, X. Li, J. Zhao, S. Bai, J. Liu and Q. Yang, *Angew. Chem. Int. Ed.*, 2012, **51**, 9164-9168.

7 Y. Zhang , J. M. Lavin and K. D. Shimizu, *J. Am. Chem. Soc.*, 2009, **131**, 12062-12063.

8 V. Stavila, R. K. Bhakta, T. M. Alam, E. H. Majzoub and M. D. Allendorf, *ACS Nano*, 2012, **6**, 9807-9817.

9 Y. Zhang, D. Song, J. C. Brown and K. D. Shimizu, *Org. Biomol. Chem.*, 2011, **9**, 120-126.

10 Y. Zhang, D. Song, L. M. Lanni and K. D. Shimizu, *Macromolecules*, 2010, **43**, 6284-6294.

11 S. R. White, N. R. Sottos, P. H. Geubelle, J. S. Moore, M. R. Kessler, S. R. Sriram, E. N. Brown and S. Viswanathan, *Nature*, 2001, **409**, 794-797.

12 K. S. Toohey, N. R. Sottos, J. A. Lewis, J. S. Moore and S. R. White, *Nat. Mater.*, 2007, **6**, 581-585.

13 Z. Zheng, X. Huang, M. Schenderlein, D. Borisova, R. Cao, H. Möhwald and D. Shchukin, *Adv. Funct. Mater.*, 2013, **23**, 3307-3314.

14 N. Roy, E. Buhler and J. M. Lehn, *Chem. Euro. J.*, 2013, **19**, 8814-8820.

15 X. Wang, F. Liu, X. Zheng and J. Sun, *Angew. Chem. Int. Ed.*, 2011, **50**, 11378-11381.

16 E. S. Gil and S. M. Hudson, *Prog. Polym. Sci.*, 2004, **29**, 1173-1222.

17 Y. Arakawa, N. Haraguchi and S. Itsuno, *Angew. Chem. Int. Ed.*, 2008, **47**, 8232-8235.

18 R. Hoogenboom, *Angew. Chem. Int. Ed.*, 2012, **51**, 11942-11944.

19 Y. Lu, Y. Mei, M. Drechsler and M. Ballauff, *Angew. Chem. Int. Ed.*, 2006, **45**, 813-816.

20 X. Wang and Y. Fu, *J. Phys. Chem. Solids*, 2008, 70, 192-196

21 S. Li, Y. Luo, M. J. Whitcombe, S. A. Piletsky, *J. Mater. Chem. A*, 2013, 1, 15102-15109.

22 S. Li, Y. Ge, A. Tiwari and S. Cao, *Small*, 2010, **6**, 2453-2459.

23 H. S. Andersson and I. A. Nicholls, *Bioorg. Chem.*, 1997, **25**, 203-211.

24 W. Wang, X. Tian, Y. Feng, B. Cao, W. Yang and L. Zhang, *Ind. Eng. Chem. Res.*, 2010, **49**, 1684-1690.

25 M. Zhu, C. Wang, D. Meng and G. Diao, *J. Mater. Chem. A*, 2013, **1**, 2118-2125.

26 L. R Wang, N. Qu and L. H. Guo, *Anal. Chem.*, 2008, **80**, 3910-3914.

Figure captions:

Scheme 1. Technical outline for the self-switchable catalysis of PtNP-S

Figure 1. The change of UV spectra as a function of TFMA/VI molar ratio (In which, TFMA (0.2 mmol mL^{-1}; 50 μ L/titration) was titrated into VI (0.03 mol mL^{-1}; 2.5 mL)

Figure 2. FTIR spectra of the prepared nanoreactors

Figure 3. TEM images of the prepared nanoreactors. a) NR-S; b) PtNR-S; c) PtNR-N

Figure 4. DLS curves of the prepared nanoreactors (In distilled water, with particles concentration of *ca.* 0. 1 μg mL^{-1})

Figure 5. Reactivity of the prepared nanoreactors for the reduction of SF (SF initial concentration, 0.01 μmol mL^{-1}; nanoreactors, 0.06 mg mL^{-1}; $NaBH_4$, 20 folds in contrast to SF)

Figure 6. Kinetic fitting of the catalytic activities of the prepared nanoreactors (SF initial concentration, 0.01 μmol mL^{-1}; nanoreactors, 0.06 mg mL^{-1})

Scheme 2. Schematic presentation of an electrochemical process with the binding molecule B

Figure 7. Reduction profiles with SF desorbing from the prepared nanoreactors (*a*: 30 ^{o}C; *b*: 50 ^{o}C) (Au working electrode, Pt counter electrodes, Ag^{+}/AgCl ref. electrode; supporting electrolyte: 0.01 mmol mL^{-1} KCl).

Table 1. Reduction potentials with SF desorbing from all nanoreactors

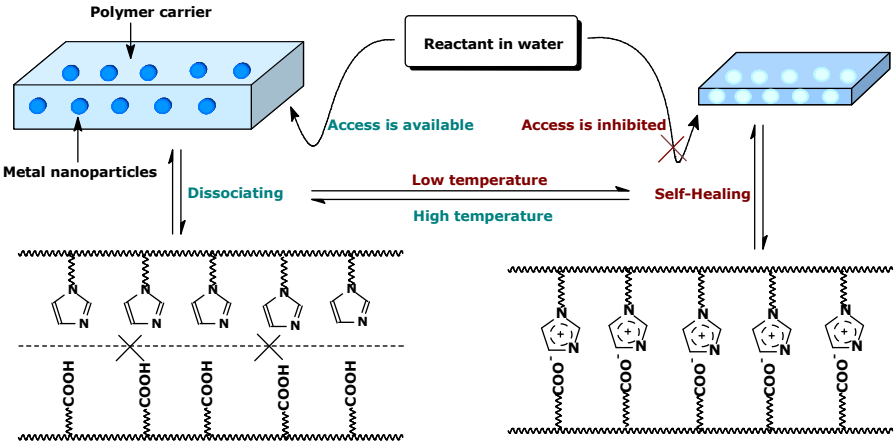

Scheme 1. Technical outline for the self-switchable catalysis of PtNP-S

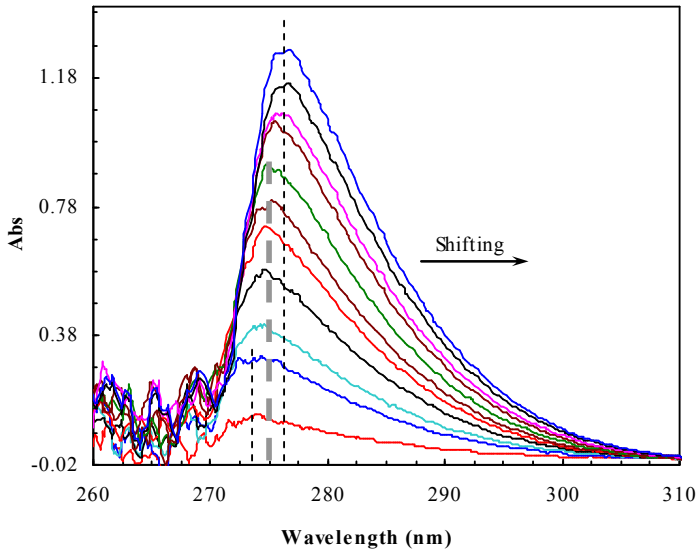

Figure 1. The change of UV spectra as a function of TFMA/VI molar ratio

(In which, TFMA (0.2 mmol mL^{-1}; 50 μ L/titration) was titrated into VI (0.03 mol mL^{-1}; 2.5 mL)

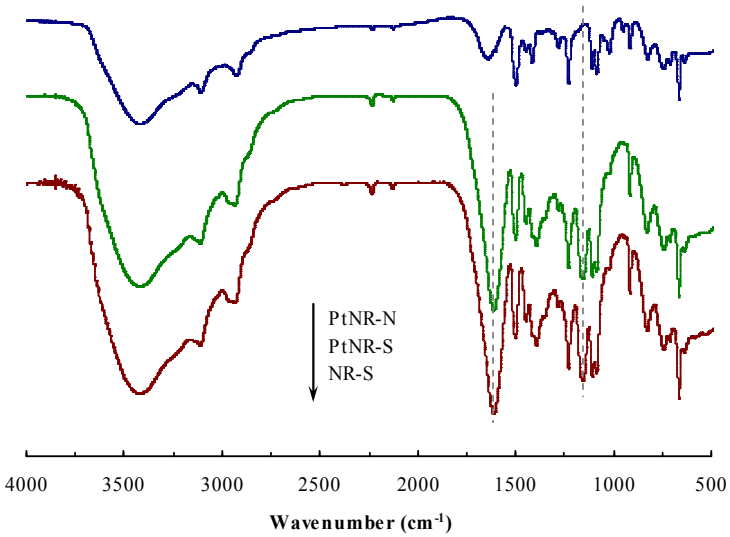

Figure 2. FTIR spectra of the prepared nanoreactors

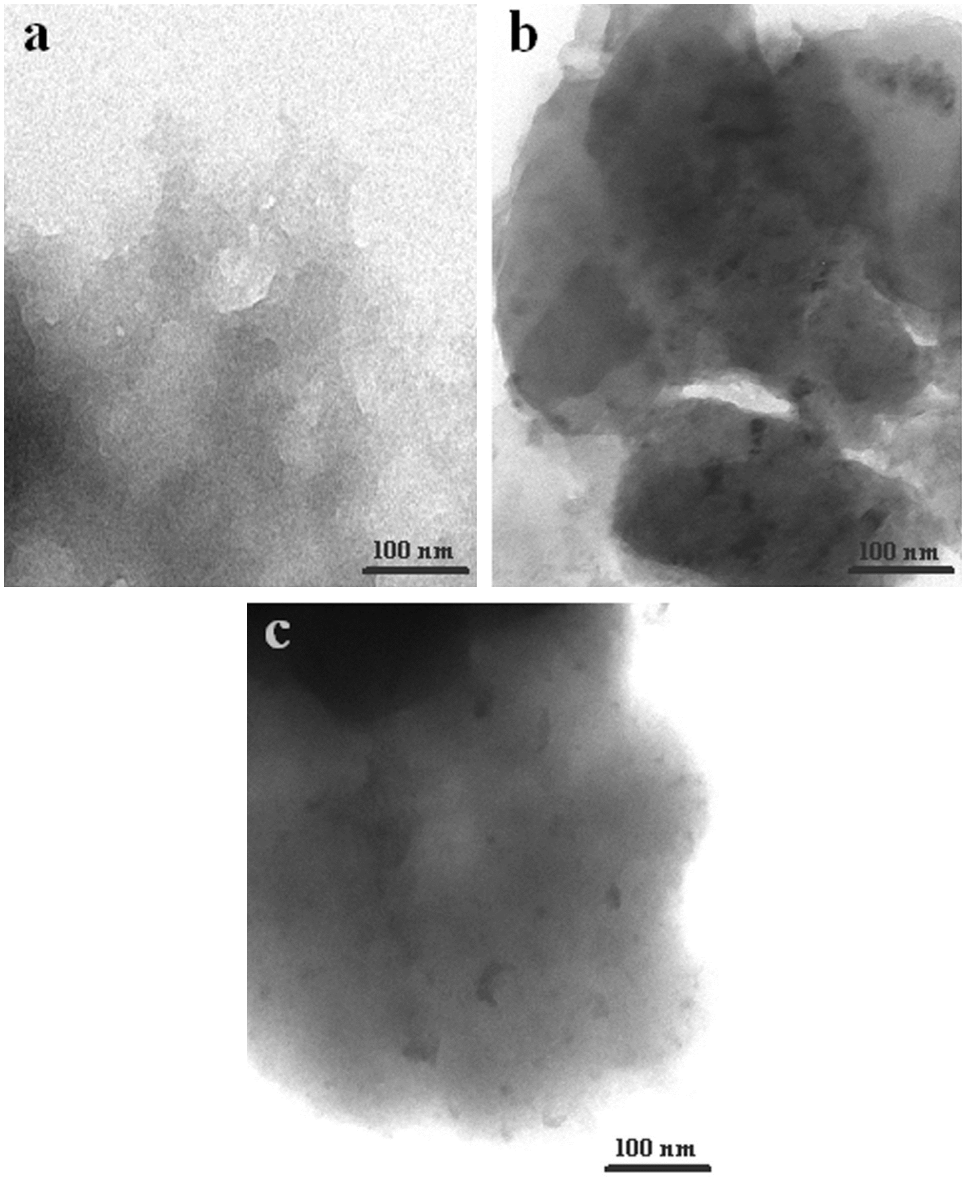

Figure 3. TEM images of the prepared nanoreactors. a) NR-S; b) PtNR-S; c) PtNR-N

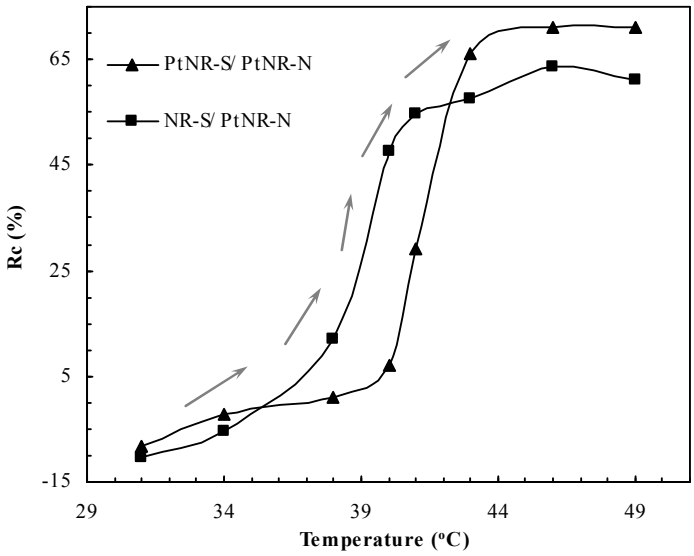

Figure 4. DLS curves of the prepared nanoreactors

(In distilled water, with particles concentration of *ca.* 0. 1 μg mL^{-1})

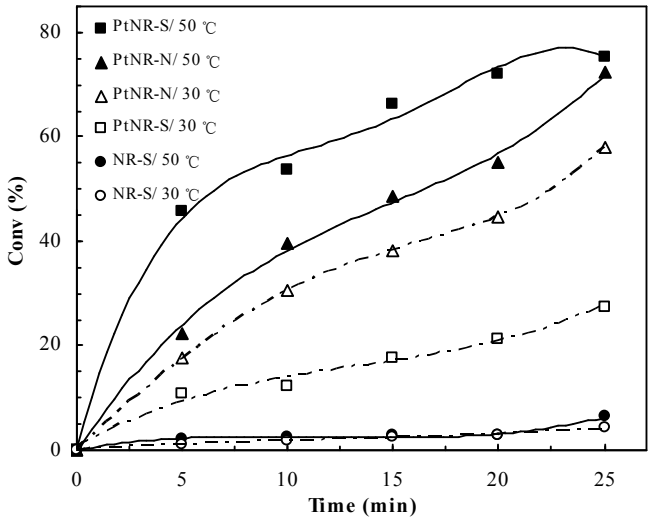

Figure 5. Catalytic activities of the prepared nanoreactors for the reduction of SF

(SF initial concentration, 0.01 μmol mL^{-1}; nanoreactors, 0.06 mg mL^{-1}; $NaBH_4$, 20 folds in contrast to SF)

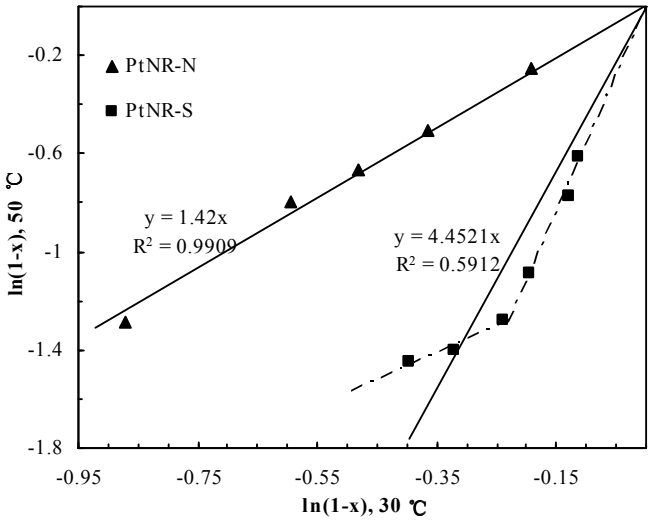

Figure 6. Kinetic fitting of the catalytic activities of the prepared nanoreactors

(SF initial concentration, 0.01 μmol mL^{-1}; nanoreactors, 0.06 mg mL^{-1})

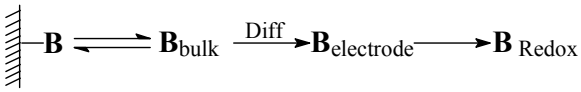

Scheme 2. Schematic presentation of an electrochemical process with the binding molecule B

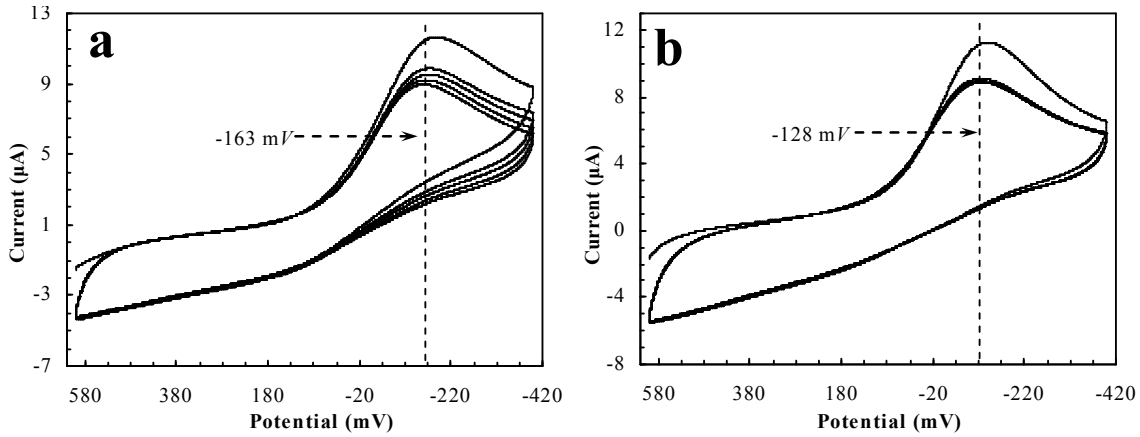

Figure 7. Reduction profiles with SF desorbing from the prepared nanoreactors (*a*: 30 °C; *b*: 50 °C) (Au working electrode, Pt counter electrodes, Ag^{+}/AgCl ref. electrode; supporting electrolyte: 0.01 mmol mL^{-1} KCl).

Table 1. Reduction potentials with SF desorbing from all nanoreactors

Nanoreactor	*Reduction potential at 30 °C (mV)*	*Reduction potential at 50 °C (mV)*	*Delta (mV)*
PtNR-S	-163	-128	35
NR-S	-161	-127	34
PtNR-N	-153	-151	2

(END)